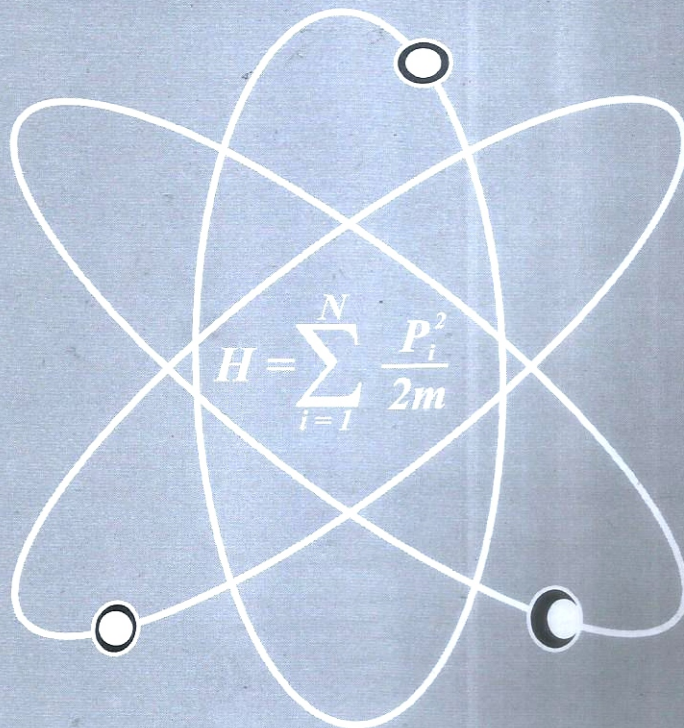


BAYERO JOURNAL OF PHYSICS AND MATHEMATICAL SCIENCES



**VOLUME 8, No. 1
SEPTEMBER, 2017.**

**Published by: THE DEPARTMENTS OF PHYSICS AND
MATHEMATICAL SCIENCES, BAYERO UNIVERSITY, KANO.**

MEMBERS OF THE EDITORIAL BOARD

- Editor in Chief:** - Prof. A. O. Musa, Dept. of Physics, Bayero University, Kano.
Asst. Editor-in-Chief 1 - Prof. U. M. Gana, Dept. of Physics, Bayero University, Kano.
Asst. Editor-in-Chief 2 - Prof. Bashir Ali, Dept. of Mathematical Sciences, B.U.K., Kano.
Circulation Editor - Prof. Garba Babaji.
Business Editor - Prof. F. S. Koki
Secretary - Mal. Usman Muhammad. Ibrahim

MEMBERS OF THE BOARD OF TRUSTEE

1. The Head of the Department of Mathematics Sciences, Bayero University, Kano.
2. The Head of Physics Department, Bayero University, Kano.
3. Member of Editorial Board.

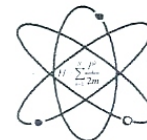
MEMBERS OF THE EDITORIAL ADVISORY COMMITTEE

1. Prof. I. H. Umar, Department of Physics, Bayero University, Kano.
2. Prof. M. Y. Bello, Department of Computer Science, Bayero University Kano.
3. Prof. A. S. Sambo, former Director-General, National Energy Commission of Nigeria, Abuja.
4. Prof. E. U. Utah, Department of Physics, University of Uyo, Akwa Ibom State.
5. Prof. B. Osazuwa, formerly of Department of Physics, Ahmadu Bello University, Zaria.
6. Prof. J. Katande, Dean at Botswana International University of Science and Technology.
7. Prof. P.N. Okeke, Department of Physics and Astronomy, University of Nigeria, Nsukka.
8. Prof. M. N. Agwu, Department of Physics, Nigerian Defence Academy, Kaduna.
9. Prof. Ado. Dan-Isa, Department of Electrical Engineering, Bayero University, Kano.
10. Dr. M. S. Abubakar, Department of Physics, Kaduna State University, Kaduna.
11. Dr. B. S. Galadanchi, Department of Electrical Engineering, Bayero University, Kano.
12. Prof. M. B. Yakasai, Department of Mathematical Sciences, Bayero University, Kano.
13. Dr. N. F. Isa, Department of Physics, Bayero University, Kano.
14. Prof. Garba Uba Goje, Dept. of Mathematical Sciences, Ahmadu Bello University, Zaria.
15. Prof. Babangida Sani, Dept. of Mathematical Sciences, Ahmadu Bello University, Zaria.
16. Dr. Y. I. Zakari, Dept. of Physics, Ahmadu Bello University, Zaria.

TABLE OF CONTENTS

Assessment of Magnetic Susceptibility on Arable Land of Kano River Irrigation Project (KRIP) Abraham Musa Zira, Aminu Ahmad Lawal, P. Sule and Oniku Adetola	1 – 8
Impedance, Dielectric And Modulus Study of Ti-doped $\text{LiSn}_2(\text{PO}_4)_3$ U. Ahmadu, K. U. Isah, A. Mann, M. I. Kimpa, and S. O. Ibrahim	9 – 21
Statistical Analysis on 2015 Nigerian Presidential Election Result S. M. Umar	22 – 29
Analysis of Structure, Microstructure and Chemical Composition of Solid Solution of Co-Doped Barium Calcium Stannatetitanate $(\text{Ba}_{1-x}\text{Ca}_x\text{Ti}_{0.975}\text{Sn}_{0.025}\text{O}_3) \cdot (0 \leq x \leq 0.12)$ U. Ahmadu, M. I. Abdulahi, Abdulwaliyu B. Usman, Uno, E. E. and Moses Agida	30 – 36
Theoretical Investigation of the Conformation, (^1H and ^{13}C) NMR Spectra and Nonlinear Optical Properties of Benzaldehyde Haidar Mas'ud Alfanda, Mansur Sa'id, and Ya'u Datti	37 – 52
Determination of Physical Properties and Proximate Analysis of Biomass Briquette Produced From Cornstalk and Waste Paper S. Namadi, A. O. Musa and A. Bala	53 – 60
Survival Times of Tuberculosis Patients an Approach to Cox (Proportional Hazard) Regression Model Damisa Adams Saddam, Abukakar Yahaya, Jamilu Garba	61 – 70
A Comparative Study of Broadside and End-Fire Linear Antenna Array Configurations Isah Ibrahim Garba and M. H. Ali	71 – 77
Fabrication and Optical Characterization of ZnO and TiO_2 Thin Film for Solar Cell Application – Abdussalam Balarabe Suleiman, Sabiu Said Abdullahi, Sabo Isiyaku and Chifu E. Ndikilar	78 – 83
An Assessment of Heavy Metals Concentration in Fish Tissues of the Wasai Dam Kano State Nigeria, Using Neutron Activation Analysis B. Haladu, N. F. Isa, B. I. Tijjani and M. U. Ibrahim	84 – 91
Calculation of Momentum Distributions of ^{14}C Core Fragment from $^{15}\text{C} + ^9\text{Be}$ Reaction Using Glauber Theory I. D. Adamu, I. S. Salisu	92 – 97
The Effect of Applied Field Stresses on The Stability of ZnO Ceramics with CaMnO_3 as Additive for Varistor Application I. I. Lakin, A. Zakaria, N. Kure, H. O. Aboh	98 – 106

Analysis of Seasonal Variation of Ionospheric Total Electron Content over Zaria, Nigeria Muhammad Usman Shehu, Rabia Salihu Said, Bello Idrith Tijjani and Umar Isah	107 – 117
Local Mode Frequencies Under Quartic Anharmonicity in 1D Monoatomic Crystals: Analytical and Numerical Study Kassim I. Lawan and G. Babaji	118 – 126
Investigation on Microstructure and Optical Properties of Cu ₂ O/ZnO Heterojunction Prepared by Screen Printing Technique Farida Mustapha, Mansur Sa'id, T. H. Darma and Haidar Mas'ud	127 - 134
Simulation of the Effect of Number of Pictures Per Group for Multi-Hypothesis Motion Compensation (MMC) in Video Sequences K. A. Busari, I. D. Adamu	135 – 142
Assessment on Impact of Hauran Wanki Pond on its Environs using Geophysical and Hydrochemical Methods in Gwale, Kano State, Nigeria Saleh. M, Maidabino, B. H. and C. O. Ologun	143 – 153
Study of Soil - Plant Heavy Metal Relations and Transfer Factor Index of Vegetable Amaranths and Sunflower in Some Selected Areas within Kano State, Nigeria Isa, N. F., U. M. Ibrahim, F. Ahmad and Y. Y. Ibrahim	154 – 166
Assessment of Some Reliability Measures of a Duplicated Standby System Subject to Individual and Group Replacement at Failure Bashir Yusuf, Sale Ali, Salisu Murtala, Ibrahim Yusuf and Abdulrahman, L. S.	167 – 179
Fabrication and Study of the Electrical Properties of Copper-Copper Sulphide (Cu-Cu ₂ S) Photoelectrochemical Solar Cell Abdu Yunusa	180 – 186
Effect of Calcium Hydroxide on the Purity of Biogas Produced from Cow Dung Ibrahim Yaro Getso and Tijjani H. Darma	187 – 194
Determination of Heavy Metals in Building Materials Used in Malumfashi Area of Katsina State, Nigeria, using Atomic Absorption Spectrometry Aku, M. O. and Yusuf, U.	195 – 200
Novel Family of Quadrature Based Iterative Methods for Nonlinear Equation using Decomposition Approach G. Ogbereyivwe and J. Emunefe	201 – 210



ANALYSIS OF STRUCTURE, MICROSTRUCTURE AND CHEMICAL COMPOSITION OF SOLID SOLUTION OF CO-DOPED BARIUM CALCIUM STANNATETITANATE ($Ba_{1-x}Ca_xTi_{0.975}Sn_{0.025}O_3$) ($0 \leq x \leq 0.12$)

U. Ahmadu¹, M. I. Abdullahi¹, Abdulwaliyu B. Usman¹, Uno, E. E¹. and Moses Agida¹

¹Department of Physics, Federal University of Technology, P. M. B. 65, Minna, Nigeria

Corresponding author: u.ahmadu@yahoo.com

ABSTRACT

$Ba_{1-x}Ca_x(Ti_{0.975}Sn_{0.025})O_3$ ($0.00 \leq x \leq 0.12$) ceramics have been synthesized by solid state reaction method. Structural analyses have been carried out to determine the effect of Ca^{2+} substitution on the structural parameters of the ceramic. The average crystallite size decreased from 36.39 nm to 35.39 nm for highly doped Ca^{2+} . Highest increase in a ratio was observed at $x = 0.06$. Microstructural evaluation of the material revealed decrease in grain size from 1 μm to 0.45 μm upon incorporation of Ca^{2+} . Energy Dispersive Spectroscopy (EDS) investigation showed variation in chemical composition but no structural transformation was observed.

Keywords: ceramic; X-ray diffraction; crystallinity; microstructure; grain size

1. Introduction

Lead-based perovskite ceramics have shown high dielectric and piezoelectric properties which are widely used in piezoelectric devices [1]. Unfortunately, the lead content in such ceramics makes it very toxic and can pollute environment causing damage to the brain and nervous system [2], hence from environmental point of view and human health protection, there is need to replace these materials with lead-free compositions. Over the years, there have been growing researches in developing lead-free piezoelectric materials which may replace their lead-based counterparts. Perovskite Barium Titanate ($BaTiO_3$ or BT) has been recognized as a promising candidate due to its potential application in multilayer ceramic capacitors, piezoelectric transducers, sensors, Fe-RAM [3], among others. BT is a typical ferroelectric which exhibits a perovskite (ABO_3) structure. However, some of its drawbacks have limited its extensive application in its pure form due to conflict between significant hysteresis in the strain and electric field dependence of the piezoelectricity of the material. These have led to difficulties in controlling the piezoelectric ceramic [3], alongside its low piezoelectric constant [4]. Thermal instability of its structural phase and other dependent properties are also of major concern. BT exhibits a relatively low transition temperature ($T_c = 120^\circ C$) at the Curie point and thus suffers structural phase transformation (ferroelectric-tetragonal to paraelectric-cubic phase) at low temperatures [5, 4]. Several attempts at improving its structural stability, ferroelectric and dielectric properties have been made [6, 7, 8]. These include the substitution of Ba^{2+} or Ti^{4+} by atoms of different sizes and oxidation states resulting in compounds of different physical and chemical properties, while still retaining the same structural phase [6, 9, 7]. It has been reported that partial substitution of Ba^{2+} by Ca^{2+} prevents grain growth, improves electromechanical properties and structural stability [10, 11, 12]. However, the substitution decreased the dielectric constant [11, 13] while the substitution of Ti^{4+} by 0.025 mol of Sn^{4+} led to increased permittivity, enhanced piezoelectric properties and decreased T_c [14]. As such, it is expected that simultaneous substitutions of Ba^{2+} by Ca^{2+} and Ti^{4+} by Sn^{4+} (0.025 mol) may offer the possibility of developing a lead-free piezoelectric ceramic. Secondary phases which affect the crystal structure amongst other properties of BT upon substitution of inappropriate Ca^{2+} concentration have been reported [11]. Therefore, the appropriate concentration of Ca^{2+} that may improve the structural phase of the ceramic is worth investigating. To the best of

our knowledge, structural and microstructural properties of BT partially substituted by Ca^{2+} and Sn^{4+} (0.025 mol) have not been investigated apart from our earlier work [15].

In the present work, the effect of Ca^{2+} substitution (on the Ba^{2+} site of BaTiO_3) on the structural and microstructural properties of $\text{Ba}_{1-x}\text{Ca}_x(\text{Ti}_{0.975}\text{Sn}_{0.025})\text{O}_3$ ceramics ($0.00 \leq x \leq 0.12$) have been investigated and the evolution of these properties with doping have been reported.

2. Experimental Procedures

$\text{Ba}_{1-x}\text{Ca}_x(\text{Ti}_{0.975}\text{Sn}_{0.025})\text{O}_3$ (BCST) ceramics (where $0.00 \leq x \leq 0.12$) were synthesized by solid state reaction method. Analytical grade BaCO_3 ($\geq 99\%$, Kermel, China.), TiO_2 and CaCO_3 (99.9 %, Qualikems, India) and SnO_2 (99.99 %, BDH, U.K) were used as the precursors. Stoichiometric amounts of these materials for the required specimens were weighed and dry-mixed thoroughly, followed by wet-mixing with distilled water as the medium. The amount of distilled water used was just enough to form slurry to prevent selective sedimentation of the reagents. The slurry was dried in an oven at 150°C for 1 h. The dried mixture was hand-ground thoroughly for homogeneity using agate mortar and pestle for 4 h. The homogenous mixture was placed in an alumina crucible and calcined at 1050°C for 4 h in a furnace to allow volatilization of by-product CO_2 . The obtained mixed powder was further ground for 1 h and granulated by adding 4 wt% polyvinyl alcohol (PVA) as binder to reduce brittleness and to have better compactness, and then pressed into 26 mm diameter and 1 mm thickness pellets at a pressure of 10 tons. Finally, the prepared pellets were sintered at 1100°C for 3 h, and furnace-cooled to obtain a crystal phase formation.

X-ray Diffractometer (D8 Advance, BRUKER AXS, 40 kV, 40 mA) with monochromatic $\text{Cu-K}\alpha$ radiation ($\lambda = 1.54060 \text{ \AA}$) was used to characterize the structural phase composition of the synthesized ceramics over a 2θ range from 20° to 90° with scan step and acquisition time of 0.034° and 88 s, respectively. The morphology and the elemental composition of the ceramics were analyzed using High Resolution Scanning Electron Microscope (HRSEM, Zeiss) coupled with EDS spectrometer working at a voltage of 20 kV with images captured at 5 kV. Prior to the analysis, the samples were placed on a carbon adhesive tape and backed on an aluminium stage. As the samples are non-conducting, a thin layer of AuPd was coated using a sputter coater and then vacuumed in the HRSEM. For measurement of the grain sizes, Imagej software was used.

3. Results and Discussion

3.1 Crystal Structure Analysis

X-ray Diffraction (XRD) patterns of the synthesized $\text{Ba}_{1-x}\text{Ca}_x(\text{Ti}_{0.975}\text{Sn}_{0.025})\text{O}_3$ ceramics ($x = 0.00, 0.06$ and 0.12) are depicted in Fig. 1. The patterns confirm that the ceramics are polycrystalline with single phase perovskite structure which compares well with JCPDS no: 00-005-0626 reference data of tetragonal BaTiO_3 . The patterns are also in agreement with the reports of other workers who prepared BT-based ceramics using similar method (Kim *et al.*, 2009; Fasasi *et al.*, 2006).

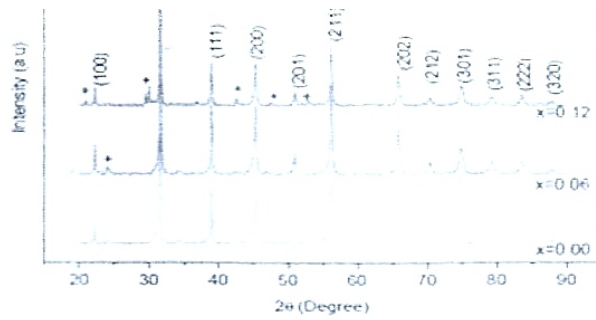


Figure 1: X-Ray Diffraction Pattern of $\text{Ba}_{1-x}\text{Ca}_x(\text{Ti}_{0.975}\text{Sn}_{0.025})\text{O}_3$ ($0.00 \leq x \leq 0.12$)

However, a minor peak around 47.5° 2θ scan was observed at $x = 0.12$ which has been identified as orthorhombic CaTiO_3 phase (Joint Commission on Powder Diffraction Standards (JCPDS) file no: 00-022-0153) and attributed to the solubility limit of Ca^{2+} in BCST. This suggests that Ca^{2+} is soluble in BCST up to 0.06 mol. There were other diffraction peaks though with very low intensities whose match could not be found as indicated in the XRD spectra. Further, it was observed that the structure sensitive peak (200) slightly shifts toward higher 2θ angles from 45.246° to 45.261° with increasing Ca^{2+} concentration. This suggests distortion of the ABO_3 unit cell lattice [16] and could lead to changes in the lattice parameters, consistent with fact that the radius of Ca^{2+} ions (0.99 \AA) is smaller than that of Ba^{2+} ions (1.34 \AA) [13].

Average crystallite size (s) were calculated by eqn. (1) [6] using the Full Width at Half Maximum (FWHM) of the most intense peak.

$$D = \frac{0.9\lambda}{\beta \cos \theta} \quad (1)$$

Where β is the FWHM of the diffraction peak expressed in radians, θ is the Bragg diffraction angle of the XRD peak, λ is the wavelength of the X-ray used which is 1.54060 \AA and D is the crystallite size in nanometers.

The calculated average crystallite size is presented in table 1 where it can be seen that the crystallite size decreased because the FWHM increased with increase in doping concentration. This is due to the fact that the smaller Ca^{2+} ions replaced the larger Ba^{2+} ions and their reactivity with the host compound decreased giving rise to decreased crystallinity.

Table 1: Ca^{2+} concentration (x in mols.), peak position (2θ) and FWHM (β) at (110) and average crystallite size (D)

x	2θ (degree)	$\beta \times 10^{-3}$ (radians)	D (nm)
0.00	31.57	3.61	36.93
0.06	31.59	3.94	33.82
0.12	31.58	3.77	35.39

Lattice parameters a and c of the ceramics were calculated from the XRD spectra using the (100), (200) and (201) diffraction peaks and compared with the JCPDS no: 00-005-0626 data of BaTiO_3 (table 2).

Table 2: Determined Lattice Constants a and c , c/a and Cell volume of $Ba_{1-x}Ca_x(Ti_{0.975}Sn_{0.025})O_3$ ceramics

x	a (Å)	c (Å)	c/a (Å)	Cell Volume (Å ³)
Referenced BT	3.994	4.038	1.0110	64.410
0.00	4.0048	4.0092	1.0011	64.30
0.06	4.0030	4.0149	1.0030	64.30
0.12	4.0020	4.0110	1.0022	64.20

It can be seen that $x = 0.00$ is weakly tetragonal in comparison with the JCPDS data of $BaTiO_3$ prepared at higher temperature. But on substitution of Ca^{2+} for Ba^{2+} , the lattice parameters a decreased while c increased and consequently c/a ratio (tetragonality) increased. However, $x = 0.06$ is seen to have the highest value and could be attributed to the solubility limit of Ca^{2+} . It has been suggested that the increase of the space available to the Ca^{2+} at the Ba^{2+} site induces ferroelectricity in dielectrics [11] and that this could be the reason for the increase in tetragonality observed on substitution of Ba^{2+} by Ca^{2+} . Also presented in table 2 is the cell volume where it is seen to slightly decrease as the concentration of Ca^{2+} increased. This has been corroborated by the shifting of the (200) peaks to higher angles with increasing Ca^{2+} concentration. Moreover, increase in c/a is a desirable characteristic of perovskite titanates because higher c/a normally increases the polarizability and the ferroelectric properties [17]. Thus the observed increase in tetragonality of $Ba_{1-x}Ca_x(Ti_{0.975}Sn_{0.025})O_3$ ($0.00 \leq x \leq 0.12$) may lead to improved ferroelectric properties. The most appropriate structural properties of $Ba_{1-x}Ca_x(Ti_{0.975}Sn_{0.025})O_3$ ceramics is obtained with $x = 0.06$.

3.2 Microstructural Analysis

Fig. 2 depicts HRSEM micrographs of $Ba_{1-x}Ca_x(Ti_{0.975}Sn_{0.025})O_3$ ($0.00 \leq x \leq 0.12$). From Fig. 2(a), it can be seen that the particles agglomerate alongside fairly homogeneous and porous microstructure.

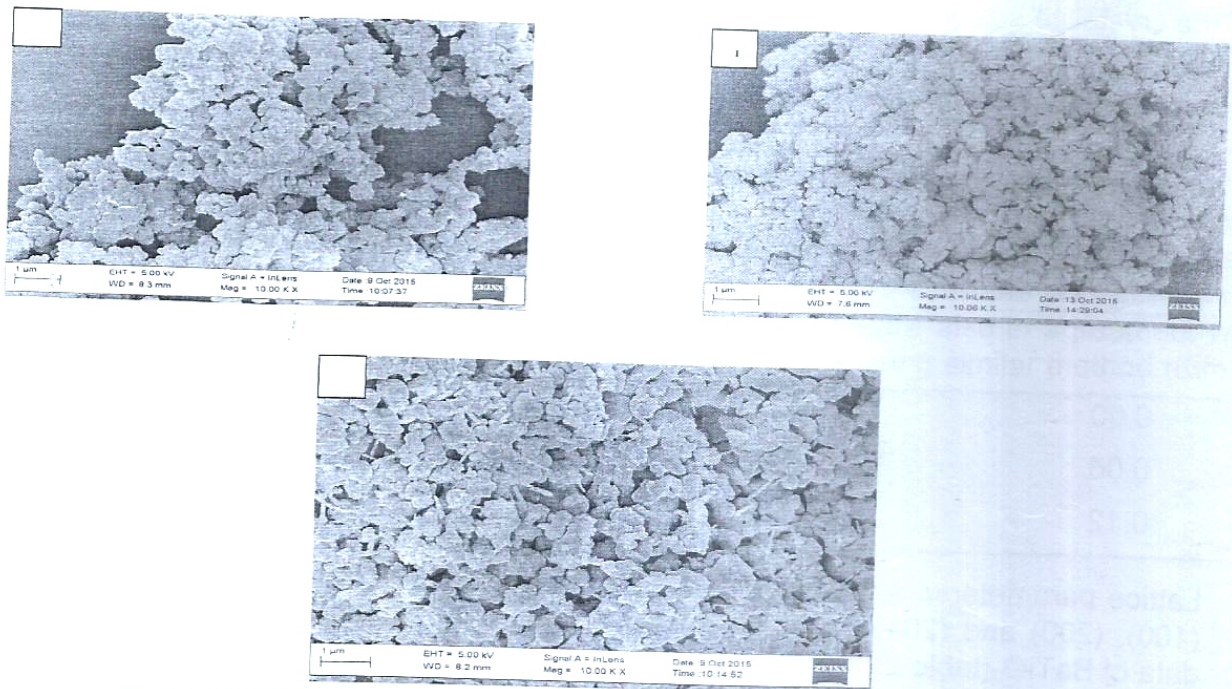


Figure 2: HRSEM micrographs of (a) $x = 0.00$ (b) $x = 0.06$ (c) $x = 0.12$

The average grain size of the ceramics is about $1\mu\text{m}$, smaller than those reported in traditional BT ceramics sintered at higher temperature ($1450\text{ }^\circ\text{C}$) [18]. The small value of grain size may be due to insufficient sintering temperature. On addition of Ca^{2+} ($x = 0.06$), closer agglomeration of grains is observed and the average grain size decreased to about $0.45\ \mu\text{m}$, eventually giving rise to the poor microstructure in Figure 2b. As Ca^{2+} concentration increased ($x = 0.12$), two regions are distinguishable in their grain size and phase compositions. The first shows a fairly fine-grained microstructure with average grain size of $0.7\ \mu\text{m}$, while the other has rod-like grains (Figure 2c) with porosity. The distinct feature of this sample is the presence of non-homogeneous microstructure. The observed rod-like grains are due to non-uniform distribution of starting powders [12]. It is generally reported that the initial powder preparation process and possibly insufficient mixing of starting powders or insufficient sintering temperature could result in poor and non-homogeneous microstructure. The decrease in average grain size of the ceramic upon substitution of Ca^{2+} for Ba^{2+} indicates that Ca^{2+} inhibits grain growth [11]. Ferroelectric properties of BT-based ceramics have been strongly linked to grain size [3] where it is found to decrease when grain size decreases. Decrease in dielectric constant may also be expected because the grain boundary is non-ferroelectric and the dielectric constant of the grain boundary is much smaller than that of the grain [9]. The smaller the grain size, the larger the grain boundary, and the lower the dielectric constant.

3.3 Chemical Composition

Fig. 3 is the Energy Dispersive (EDS) spectrum showing the elemental compositions of $\text{Ba}_{1-x}\text{Ca}_x(\text{Ti}_{0.975}\text{Sn}_{0.025})\text{O}_3$ ceramics. All the peaks have been identified with the corresponding elements that match that peak. The spectra clearly reveal the presence of Ba, Ca, Ti, Sn, O, C, Au and Pd, except in the case of $x = 0.00$ (Fig. 3a) where Al is evident.

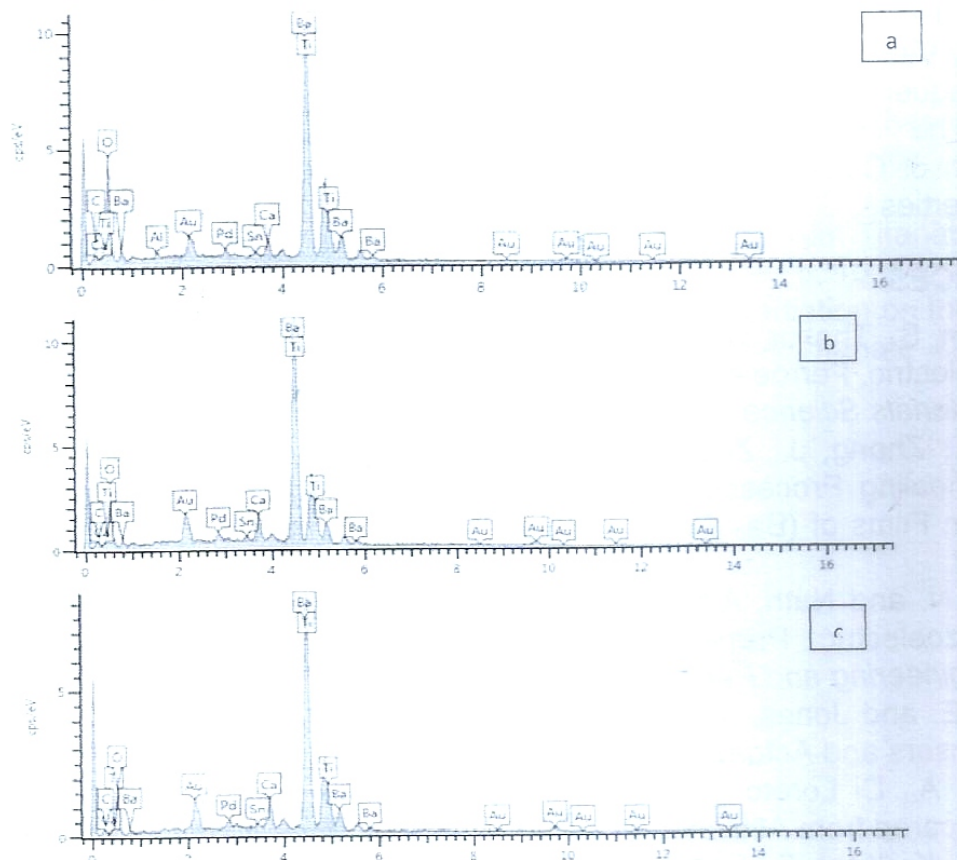


Fig. 3: EDS spectrum of (a) $x = 0.00$ (b) $x = 0.06$ (c) $x = 0.12$

The C(carbon) source may have come from the carbon tape. AuPd (Gold-Paladium) is present in the compound in order to make it conducting; while the Al may be attributed to contamination during the preparation of samples for SEM analysis. Table 3 gives a quantitative comparison of the nominal compositions and the normalized EDS-derived composition, where the major sources of error have been removed and the remaining elements normalized to 100% to give a representation of the elements present in the compound. The variations in the normalized EDS derived composition in comparison with the nominal composition could be assigned to deficiency of oxygen during sintering in the ambient. The overlap of Ba and Ti is clear in the spectra and makes it difficult to distinguish between them in the quantification results, an observation that has been reported by other workers. However, further investigations are required to elucidate the higher values of the normalized EDS derived results.

Table 3. Nominal and Normalized EDS-derived elemental composition

Sample (x)	Nominal Composition (atomic %)						Normalized EDS Derived Composition (atomic %)					
	Ba	Ca	Sn	Ti	O	Total	Ba	Ca	Sn	Ti	O	Total
0.00	20.00	-	0.50	19.50	60.00	100	18.41	-	0.33	19.11	62.15	100
0.06	18.80	1.20	0.50	19.50	60.00	100	19.59	3.59	0.63	22.97	52.69	100
0.12	17.60	2.4	0.50	19.50	60.00	100	22.31	4.7	0.4	26.64	45.95	100

4. Conclusion

Polycrystalline $\text{Ba}_{1-x}\text{Ca}_x(\text{Ti}_{0.975}\text{Sn}_{0.025})\text{O}_3$ ($0.00 \leq x \leq 0.12$) ceramics were prepared by solid state reaction method. The results indicate that the FWHM increased, crystallite size and grain size decreased as the concentration of Ca^{2+} increased, all of which lead to reduced crystallinity. Variations are observed in the lattice parameters which cause lattice distortion and consequently lead to increase in c/a ratio alongside slight contraction of unit cell volume. The changes in the structural and microstructural properties observed on substitution of Ca^{2+} for Ba^{2+} in BCST ceramic could lead to changes in the dielectric and other properties.

REFERENCES

- [1] Mahajan, S., Thakur, O. P., Prakash, C. and Sreenivas, K. (2011). Effect of Zr on Dielectric, Ferroelectric and Impedance Properties of BaTiO_3 Ceramic. *Bulletin of Materials Science*, **34**, 7, 1483–1489.
- [2] Shi, M., Zhong, J., Zuo, R., Xu, Y., Wang, L., Su, H. and Gu, C. (2013). Effect of Annealing Processes on the Structural and Electrical Properties of the Lead-free Thin Films of $(\text{Ba}_{0.9}\text{Ca}_{0.1})(\text{Ti}_{0.9}\text{Zr}_{0.1})\text{O}_3$. *Journal of Alloys and Compounds*, **562**, 116–122.
- [3] Medhi, N. and Nath, A.K. (2013) Gamma Ray Irradiation Effects on Ferroelectric and Piezoelectric Properties of Barium Titanate Ceramics. *Journal of Material Engineering and Performance*, **22**, 2716-2722.
- [4] Aksel, E. and Jones, J. L. (2010). Advances in Lead-Free Piezoelectric Materials For Sensors and Actuators. *Sensors*, **10**, 1935-1954.
- [5] Frattini, A., Di Loreto, A., de Sanctis, O. and Benavidez, E. (2012). BCZT Ceramics Prepared from Activated Powders. *Procedia Material Science*, **1**, 359-365.
- [6] Dash, S. K., Kant, S., Danlai, B., Swain, M. D. and Swain, B. B. (2014). Characterization and Dielectric Properties of Barium Zirconium Titanate Prepared by Solid State Reaction and High Energy Ball Milling Processes. *Indian Journal of Physics*, **88**, 2, 129-135.

- [7] Kumar, Y., Mohiddon, A. Md., Srivastava, A. and Yadav, K. L. (2009). Effect of Ni Doping on Structural and Dielectric Properties of BaTiO₃. *Indian Journal of Engineering & Material Sciences*, **16**, 390-394.
- [8] Wodecka-Duś, B., Lisińska-Czekaj, A., Orkisz, T., Adamczyk, M., Osińska, K., Kozielski, L. and Czekaj, D. (2007). The Sol-gel Synthesis of Barium Strontium Titanate. *Materials Science-Poland*, **25**, 3, 719-799.
- [9] Cai, W., Fu, C. L., Gao, J. C. and Zhao, C. X. (2011) Dielectric Properties and Microstructure of Mg doped barium titanate ceramics. *Adances in Applied Ceramics*, **110**, 3, 181-185.
- [10] Matsuura, K., Hoshina, T., Takeda, H., Sakabe, Y. and Tsurumi, T. (2014). Effects of Ca Substitution on Room Temperature Resistivity of Donor-doped Barium Titanate Based PTCR Ceramics. *Journal of the Ceramic Society of Japan*, **122**, 6, 402-405.
- [11] Choi, Y.K., Hoshina, T., Takeda, H. and Tsurumi, T. (2010) Effects of Ca and Zr Additions and Stoichiometry on the Electrical Properties of Barium Titanate-based Ceramics. *Journal of the Ceramic Society of Japan*, **118**, 10, 881-886.
- [12] Paunovic, V., Zivkovic, Z., Vracar, L., Mitic, V. and Miljkovic, M. (2004) The effect of additive on microstructural and electrical properties of BaTiO₃. *Serbian Journal of Electrical Engineering*, **1**, 3, 89-98.
- [13] Yun, S., Wang, X., Li, B. and Xu, D. (2007). Dielectric Properties of Ca-substituted Barium Strontium Titanate Ferroelectric Ceramics. *Solid State Communications*, **143**, 461-465.
- [14] Nath, A. K. and Medhi, N. (2012). Density Variation and Piezoelectric Properties of Ba(Ti_{1-x}Sn_x)O₃ Ceramics Prepared from Nanocrystalline Powders. *Bulletin of Materials Science*, **35**, 5, 847-852.
- [15] Ahmadu Umaru, Ahmad Abubakar Soje, Abdulwaliyu Bidemi, Muhammad Auwal Musa, Isah Kasim Uthman. (2016). Structural and Microstructural Study of Gamma Ray--Irradiated Co-doped Barium Titanate (Ba_{0.98}Ca_{0.12}Ti_{0.975}Sn_{0.025}O₃). *Processing and Application of Ceramics*, **10** (2):79-85.
- [16] Chen, Z. and Yuan-fang, Q. U. (2012) Dielectric Properties and Phase Transitions of La₂O₃- and Sb₂O₃-doped Barium Strontium Titanate Ceramics. *Transactions of Nonferrous Metals Society of China*, **22**, 2742-2748.-I
- [17] Mady, H. A. (2011). XRD and Electric Properties of Lead Barium Titanate Ferroelectric Ceramic. *Australian Journal of Basic and Applied Sciences*, **5**, 10, 1472-1477.
- [18] Nath, A. K. and Medhi, A. (2014). Effect of Gamma Ray Irradiation on the Piezoelectric and Ferroelectric Properties of Bismuth Doped Barium Titanate Ceramics. *Indian Journal of Physics*, Doi:10.1007/s12648-014-0531-5.